Published in final edited form as:
Exp Neurol. 2010 July ; 224(1): 197–206. doi:10.1016/j.expneurol.2010.03.011.

Transcriptome analysis of a tau overexpression model in rats implicates an early pro-inflammatory response

David B. Wang[a,b], **Robert D. Dayton**[a], **Richard M. Zweig**[c], and **Ronald L. Klein**[a,b]

[a]Department of Pharmacology, Toxicology and Neuroscience, Louisiana State University Health Sciences Center, Shreveport, LA 71130, USA

[b]Gene Therapy Program, Louisiana State University Health Sciences Center, Shreveport, LA 71130, USA

[c]Department of Neurology, Louisiana State University Health Sciences Center, Shreveport, LA 71130, USA

Abstract

Neurofibrillary tangles comprised of the microtubule-associated protein tau are pathological features of Alzheimer's disease and several other neurodegenerative diseases, such as progressive supranuclear palsy. We previously overexpressed tau in the substantia nigra of rats and mimicked some of the neurodegenerative sequelae that occur in humans such as tangle formation, loss of dopamine neurons, and microgliosis. To study molecular changes involved in the tau-induced disease state, we used DNA microarrays at an early stage of the disease process. A range of adeno-associated virus (AAV9) vector doses for tau were injected in groups of rats with a survival interval of two weeks. Specific decreases in messages for dopamine related genes validated the technique with respect to the dopaminergic cell loss observed. Of the mRNAs upregulated, there was a dose-dependent effect on multiple genes involved in immune response such as chemokines, interferon-inducible genes and leukocyte markers, only in the tau vector groups and not in dose-matched controls of either transgene-less empty vector or control green fluorescent protein vector. Histological staining for dopamine neurons and microglia matched the loss of dopaminergic markers and upregulation of immune response mRNAs in the microarray data, respectively. RT-PCR for selected markers confirmed the microarray results, with similar changes found by either technique. The mRNA data correlate well with previous findings, and underscore microgliosis and immune response in the degenerative process following tau overexpression.

Keywords

adeno-associated virus; neurodegenerative diseases; microarray; microtubule-associated protein tau; gene transfer; immune response; gliosis; progressive supranuclear palsy

Corresponding author: David B. Wang, Department of Pharmacology, Toxicology and Neuroscience, Louisiana State University Health Sciences Center, Shreveport, LA 71130, USA, 318-675-7833, Fax 318-675-7857, DWang@lsuhsc.edu.

Introduction

A number of neurodegenerative diseases are characterized by microtubule-associated protein tau pathology, or tauopathy, such as Alzheimer's disease (AD), frontotemporal dementia and parkinsonism linked to chromosome 17 (FTDP-17), progressive supranuclear palsy (PSP), and corticobasal degeneration (CBD). There are a range of clinical symptoms across the tauopathy diseases including dementia, changes in personality, parkinsonism, aphasia and speech apraxia, and signs of bulbar degeneration (Kumar-Singh & Van Broeckhoven, 2007; Ludolph et al., 2009). While neurofibrillary tangles are an end stage, post-mortem marker, the earlier stage neuropathology and dysfunction of tau may initially trigger the degenerative process. Disruption in tau's dynamic phosphorylation-dependent interaction with microtubules, leading to hyperphosphorylated tau and small oligomer formation, may destine the neuron to tangles and death later on (Buée et al., 2000; Golde, 2006; Gendron and Petrucelli, 2009 for review). We viewed mRNA changes at an early stage in tau-induced neurodegeneration in a rat model to make hypotheses about early events in tau's neurodegenerative mechanism, before all the neurons are lost, in hopes of speculating a preventative strategy.

Delivery of the human tau gene directly to the rat substantia nigra (SN) yields a range of neuronal loss that is time- and dose-dependent, and regulated by the animal's age and the efficiency of gene transfer (Klein et al., 2008; 2009). The SN is relevant for diseases involving tau pathology and neurofibrillary tangles where there is degeneration of the pigmented dopamine neurons and the potential for parkinsonism, such as PSP (Poorkaj et al., 2002), FTDP-17 (Mirra et al., 1999), and CBD (Wakabayashi et al., 1994; Di Maria et al., 2000). Tauopathy is also prevalent in the SN in AD (Schneider et al., 2002). The SN in the rat is small and therefore provides a facile index for loss of a specific neuronal population. The tau overexpression in rats with the adeno-associated virus (AAV) vector produces mature neurofibrillary tangles viewed by electron microscopy or Gallyas staining (Klein et al., 2005), although the number of confirmed neurons with tangles is small relative to the number of neurons expressing hyperphosphorylated tau, or the number of dopaminergic neurons that are lost. Since the hyperphosphorylated tau expression (i.e., pre-tangle pathology) matches better with degree of the neuronal loss, the rat model is a good way to study neuron loss induced by early stage tau pathology. With control over tau vector expression onset, a gradient of intensity of the tau disease state can be produced to mimic either early or later stages.

Here, we inspected an early time in the tau vector induced disease state for mRNA profiles. We tested for differences between a tau group and a control green fluorescent protein (GFP) group, and also compared changes at three tau vector doses. Other controls included sham vehicle and empty vector to attribute message changes specifically due to tau overexpression, and hopefully enrich our knowledge about the tau disease process. Histological analysis after tau gene transfer to the SN of either young or aged rats (Klein et al., 2009) suggested that microgliosis was an early and possibly causative event in the ensuing loss of dopaminergic neurons. Both microgliosis and neuron loss were augmented in aged rats, with the peak microgliosis preceding the peak cell loss. The microgliosis in the rat model could be relevant to microgliosis in tau diseases such as PSP (Ishizawa et al., 2000); its early occurrence in the degenerative sequence is consistent with tau transgenic mice where tangles formed after microgliosis (Yoshiyama et al., 2007). We therefore hypothesized that mRNAs for markers of microgliosis and inflammation, such as pro-inflammatory cytokines and their receptors, would be specifically elevated by tau at an early stage of the disease state, and that mRNAs for dopaminergic markers would be lost in a tau vector dose-dependent manner.

Materials and Methods

Vectors and injections

AAV9 vectors for human wild type tau including exons 2, 3 and 10 (the longest form of tau), GFP control, or empty control with no transgene, were prepared as described (Klein et al., 2009). The expression cassette included AAV2 terminal repeats, the cytomegalovirus/chicken beta-actin promoter, and a polyadenylation sequence. The AAV purification method involved transfecting 293-T cells, harvesting and lysing the cells 3 days later, running an iodixanol gradient, washing and concentrating on filter units, sterilizing through a syringe tip, aliquoting, and freezing (Klein et al., 2009). The AAV9s were dose matched by diluting with lactated ringer's buffer, the vehicle solution. Preps were titered for vector genomes (vg)/ml by a dot-blot method. Samples from each prep were directly loaded on protein gels and immunoblotted with an AAV capsid monoclonal antibody B1 from Meridian (Saco, ME; 1:750), to confirm the dot-blots and ensure equal dosing.

Male Sprague-Dawley rats (3 months of age, from Harlan, Indianapolis, IN) were anesthetized intramuscularly with a 1 ml/kg cocktail containing 3 ml xylazine (20 mg/ml, from Butler, Columbus, OH), 3 ml ketamine (100 mg/ml, from Fort Dodge Animal Health, Fort Dodge, IA), and 1 ml acepromazine (10 mg/ml, from Boehringer Ingelheim, St. Joseph, MO). Virus (3 μl) was injected with a 27-gauge cannula connected via 26-gauge polyethylene tubing to a 10 ul Hamilton syringe mounted to a microinjection pump (CMA/Microdialysis, North Chelmsford, MA) at a rate of 0.25 μl/min on one side of the brain. Stereotaxic coordinates for the SN were 5.3 P, 2.1 L, and 7.6 V (Paxinos and Watson, 1998). The needle remained there for an additional minute before being slowly withdrawn from the animal (over 2 min). The skin was then sutured and the animal placed on heating pads until conscious before being returned to its cage. All procedures were done in accordance with our institutional ACUC and the NIH Guide for Care and Use of Laboratory Animals.

Treatment groups, dosing, and comparisons

There were three vector groups, tau, GFP, empty, and a sham vehicle injection group, with five rats per groups. Tau or GFP were applied at two equal doses 2.4×10^9 and 1.2×10^{10} vg, and the empty vector was applied at the 1.2×10^{10} vg dose. The tau vector was also used at a higher dose, 3.6×10^{10} vg; this group had only four rats. We attempted to pinpoint an early stage in the disease process with low to mid range doses of the tau vectors and an interval of 2 weeks. We chose the lowest tau vector dose to produce a baseline of expression without lesion, based on previous doses (Klein et al., 2009). At the higher doses of the tau vector, we targeted stronger lesioning effects. Another study with AAV9 tau showed that losses in striatal dopamine content begin to occur by 2 weeks (Klein et al., 2008). By studying a 15-fold range of tau vector doses at 2 weeks, we aimed to generate mild to mid level disease states.

We were most interested in comparing tau versus GFP at the mid dose (1.2×10^{10} vg), with the tau, but not the GFP, vector causing a partial dopaminergic lesion. The low dose of either tau or GFP (2.4×10^9 vg) was not expected to cause as many changes either histologically or by microarray, and served as a baseline. While GFP controls for the purpose of expressing a foreign transgene other than tau, an empty vector could avoid GFP-specific effects, so we also analyzed tau versus empty at the mid dose. Next, we looked for dose-dependent effects, comparing the 3 doses of tau against the vehicle solution. Other comparisons were of interest, such as GFP versus empty (GFP effects), and empty versus vehicle (AAV effects).

The tau expression and effects on dopaminergic markers and microglia were viewed in sister animals (2 per group), using described immunohistochemistry methods (Klein et al., 2009).

We monitored markers for dopaminergic neurons (tyrosine hydroxylase, TH; Pel-Freez, Rogers, AR, 1:2000), human tau (E1, provided by Leonard Petrucelli, Mayo Clinic, Jacksonville, FL, 1:2000), and hyperphosphorylated tau (CP13, provided by Peter Davies, Albert Einstein College of Medicine, New York, NY, 1:2000) in sister animals at 2 weeks, and for microglia (Cd11b, Chemicon, Temecula, CA, 1:1000) and astroglia (glial fibrillary acidic protein, GFAP, Chemicon, 1:1000) over a 14 day time-course (1, 3, 7, 14 days). Because microgliosis appears to be an early and therefore perhaps causative phenomenon in the tau vector induced disease state, which we predicted to be evidenced in mRNA profiles, we viewed immunoreactivity for microglia at intervals preceding the microarray in tau vector and control rats.

Microarray and statistics

Two weeks after gene transfer, the SN was dissected with the aid of a brain block and biopsy punch (both from World Precision Instruments, Sarasota, FL) and stored in 1 ml of RNA*later* (Ambion, Austin, TX) overnight at 4°C. Tissue was homogenized in 1 ml RNA STAT-60 (Tel-Test Inc, Friendswood, TX). RNA was extracted with chloroform/ isopropanol, washed with ethanol, and dissolved in RNase-free water (Ambion). RNA was then further purified using the RNeasy MinElute Cleanup Kit (Qiagen, Valencia, CA) and stored at -80°C.

RNA concentration was measured using a spectrophotometer while integrity was assessed by electrophoresis on the Agilent 2100 Bioanalyzer (Agilent Technologies, Palo Alto, CA). Double-stranded cDNA was synthesized from approximately 7 μg total RNA using a Superscript cDNA Synthesis Kit (Invitrogen, Carlsbad, CA) in combination with a T7-$(dT)_{24}$ primer. Biotinylated cRNA was transcribed *in vitro* using the GeneChip IVT Labeling Kit (Affymetrix, Santa Clara, CA) and purified using the GeneChip Sample Cleanup Module (Affymetrix). Purified cRNA (20 μg) was incubated in fragmentation buffer (200 mM Tris-acetate, pH 8.1, 500 mM potassium acetate, 150 mM magnesium acetate) at 94°C for 35 minutes and chilled on ice. Fragmented biotin-labeled cRNA (10 μg) was hybridized to the Rat Genome 230 2.0 Array (Affymetrix), interrogating 31,099 rat genes. Arrays were incubated for 16 hr at 45°C with constant rotation (60 rpm), washed and then stained for 10 min at 25°C with 10 μg/ml streptavidin-R phycoerythrin (Vector Laboratories, Burlingame, CA) followed by 3 μg/ml biotinylated goat anti-streptavidin antibody (Vector Laboratories) for 10 minutes at 25°C. Arrays were scanned using an Affymetrix GeneChip Scanner 3000 7G. Pixel intensities were measured, expression signals were analyzed and features extracted, mined, and exported using the manufacturer's software packages.

Arrays were globally scaled to a target intensity value of 2500 in order to compare individual experiments. Whether each mRNA was present in each sample, as well as the direction of change, and fold change of gene expressions between samples were determined by the software. Statistical analyses were performed with GeneSifter™ software (http://www.genesifter.net). Individual pairs of dose-matched groups were compared by student t-tests with Benjamini and Hochberg correction for multiple comparisons.

RT-PCR

RT-PCR was performed using the Taqman Universal PCR Master Mix with the 7900HT Real-Time PCR System (Applied Biosystems, Foster City, CA) to confirm microarray results. cDNA was transcribed from 1 ug of RNA using the iScript cDNA Synthesis Kit (Invitrogen, Carlsbad, CA) and stored at -20°C. Cycling parameters were 50°C for 2 minutes, 95°C for 10 minutes, and 40 cycles of 95°C for 15 seconds then 60°C for 1 minute. Reactions were run in triplicate in a 96-well fast optical plate (Applied Biosystems) and

contained 20 ng of cDNA along with 1 μl of 20× primer/probe from the Taqman Gene Expression Assays (Applied Biosystems) for each gene probed. These included: interleukin 1-beta (IL1B; Catalog number Rn00580432_m1), tumor necrosis factor (TNF; Rn99999017_m1), RT1 class II locus Db1 (RT1-Db1; Rn01429350_m1), solute carrier family 6 (neurotransmitter transporter, dopamine) member 3 (SLC6A3; Rn00562224_m1), and TH (Rn00562500_m1). Glyceraldehyde 3-phosphate dehydrogenase (GAPDH; Rn99999916_s1) was used as a housekeeping gene. Primer/probe pairs were purchased from Applied Biosystems. Ct (cycle threshold) values were generated by the software, and represent the cycle time it takes for the fluorescence to reach a designated threshold (up the linear portion of the sigmoidal PCR amplification); the more starting mRNA for that specific probe there is, the lower the Ct value. Data for each specific target is represented as ΔCt, the Ct value of the housekeeping gene GAPDH minus that of the specific target. Thus, while all ΔCt values are negative due to the relatively large amount of GAPDH mRNA (low Ct value) compared to the target mRNAs (higher Ct value), an increase in the ΔCt in treated groups signifies an increase in target mRNA amount.

Results

Quality control for viral protein

We compared amounts of viral capsid proteins in the preps to confirm equal dosing based on dot-blot titers of encapsidated DNA. Each AAV showed bands of consistent size (60-90 kDa) and stoichiometry (1:1:20) for VP1, VP2, and VP3 proteins. The B1 antibody detected the empty vector, AAV9 GFP, and AAV9 tau equally well, and different doses of each vector stained at different intensities accordingly (Fig. 1). The dot-blot titers for vector DNA matched well for levels of capsid proteins (equal vector genome comparisons in consecutive lanes on the right side of Fig. 1). There were lower molecular weight bands, which we assume to be degradation products, in all of the preps.

mRNA profiles after tau or GFP gene transfer

To identify differentially expressed messages in the SN of rats overexpressing tau, we used Affymetrix rat genome microarray chips to probe changes in 31,099 different mRNAs or expressed sequence tags. The groups (n=5) were set up as follows: lactated ringers vehicle, empty transgene-less AAV9 (1.2×10^{10} vector genomes), and 2 groups of dose-matched AAV9 GFP or AAV9 tau (2.4×10^{9} or 1.2×10^{10} vector genomes). A third dose of AAV9 tau (3.6×10^{10} vector genomes) was also studied (n=4). A two week time-point was chosen to reflect changes occurring early in the neurodegenerative process, before maximal loss of neurons occur. Overexpression of tau or GFP did not change the overall number of messages detected in the rat SN relative to all of the probes present on the array, as approximately 55-60% of the total array were detected in each group (not shown). Direct comparisons between selected groups were made using the student's t-test with Benjamini and Hochberg correction. Differences in expression of at least 2-fold in either direction with P value < 0.05 were treated as significant.

We probed for potential effects specific to the virus or the GFP using several controls (vehicle injections, empty AAV9 and AAV9 GFP). Comparing vehicle to the empty AAV9 vector, only 24 messages were affected (10 mapped to known genes), with upregulation of 11 and downregulation of 13, the greatest effect a 3.35 fold decrease (osteoglycin, a bone associated glycoprotein). No increases in messages related to immune response were seen. AAV9 GFP, when compared to the empty vector at an equal dose of 1.2×10^{10} vg, produced more changes: 228 messages changed (142 mapped to identified genes), upregulating 80 and downregulating 148, with the greatest effect a 31.85 upregulation of forkhead box g1

(Foxg1), a transcription factor involved in brain development (Martynoga et al., 2005). The data suggest more changes due to GFP than the AAV9 under these conditions.

At the lowest dose of tau and GFP vectors (2.4×10^9 vg), tau produced few effects compared to GFP. Only 10 messages (5 mapped to identified genes) were altered when compared to AAV9 GFP, with 5 being upregulated and 5 downregulated and the largest change a 3.46 fold decrease. The identified messages and change in the tau group relative to GFP were as follows: killer cell lectin-like receptor, subfamily D, member 1, down 3.46-fold; discoidin domain receptor tyrosine kinase 2, down 2.57-fold; budding uninhibited by benzimidazoles 1 homolog, down 2.29-fold; forkhead box S1, up 2.44-fold; and spermatogenesis associated 2-like, up 2.22-fold. Message changes seen at this lowest dose were dissimilar from those at the higher doses, perhaps consistent with a lack of lesioning effect from the lowest dose of tau.

The middle dose of AAV9 tau was compared to AAV9 GFP (1.2×10^{10} vg). Compared to GFP, the middle dose of tau vector resulted in 299 message changes (166 mapped to known genes), with the majority of them (216) upregulated. The top 50 changes based on intensity are listed in Table 1, with the cutoff being a 2.73-fold change. The list is completed for all significant changes over 2-fold in Supplemental Table 1. Of the 166 message changes mapped to known genes, 47/166 (28.3%) were genes involved in immune response, including the most affected message, a 16.05-fold upregulation in chemokine (C-X-C motif) ligand 10 (Cxcl10), involved in T-cell generation and trafficking (Dufour et al., 2002). Forty four of the forty seven immune related messages were upregulated, signifying a pro-inflammatory response to tau. Other messages increased by tau were comprised of transcription factors (16/166, 9.6%) such as activating transcription factor 3 (Atf3) involved in neuronal stress response and survival (Song et al., 2008), cytoskeletal proteins (14/166, 8.4%) such as the microtubule subunits beta 4 and beta 6 tubulin (Tubb4, Tubb6), cell cycle regulation (8/166, 4.8%) such as the cell cycle inhibitor cyclin-dependent kinase inhibitor 1A (Cdkn1a, also known as p21; Delobel et al., 2006), and protein degradation (6/166, 3.6%) such as ubiquitin conjugating enzymes E2L 6 and E2N (Ube2l6, Ube2n) and proteasome subunit beta 9 (Psmb9; Oddo, 2008 for review). Decreased messages were comprised of synaptic proteins (5/166, 3%) such as alpha-synuclein (Snca) and synaptotagmin I (Syt1), receptors (3/166, 1.8%) such as cholinergic receptors, nicotinic, alpha 5&6 (Chrna5, Chrna6), and transporters (3/166, 1.8%) such as solute carrier family 6 (neurotransmitter transporter, dopamine) member 3 (Slc6a3, also known as dopamine transporter, or DAT). Markers of dopaminergic neurons, such as tyrosine hydroxylase (TH) and dopa decarboxylase (Ddc), were hypothesized to decrease due to tau, but did not show up in the comparison against GFP. AAV9 tau only decreased these mRNAs 1.51 and 1.77-fold, respectively when compared to AAV9 GFP. One of the messages for cytoskeletal proteins was for endogenous rat tau, which was increased in the tau group compared to GFP by 2.30-fold. Based on the hybridization probes used in the microarray, we are confident that the increase did not incorporate the recombinant human tau mRNA from the vector. We therefore re-examined the data and found a 1.89-fold decrease in rat tau in the GFP group relative to the empty vector ($P < 0.05$), which likely explains the lowered rat tau message in the GFP group compared to the tau group, and indicates a specific side effect of the GFP.

AAV9 tau was also compared to a dose-matched, transgene-less empty AAV9 vector. AAV9 tau produced fewer changes here than when compared to the AAV9 GFP group. AAV9 tau produced 137 changes (90 mapped to known genes), and similarly, the majority were upregulated (115). The top 50 changes based on intensity are listed in Table 2, with the cutoff being a 2.36-fold change. The list is completed for all significant changes over 2-fold in Supplemental Table 2. Of the 90 messages, again the majority were increases in messages involved in immune response, accounting for 54/90 (60%) of total changes, including the

biggest change, a 16.3-fold upregulation in antigen presentation molecule RT1-Aw2 (Rolstad et al., 1997 for review). Other messages increased by tau were similar to changes seen when compared to GFP, and fell into cell cycle regulation (8/90, 8.9%) such as p21, protein degradation (4/90, 4.4%) such as ubiquitin-conjugating enzyme E2L 6 (Ube2l6) and proteasome subunits beta type 8 & 9 (Psmb8, Psmb9), and protein chaperones (3/90, 3.3%) such as heat shock protein 1 (Hspb1, also known as Hsp27). Messages decreased by tau were either transporters (6/90, 6.7%) such as DAT and solute carrier family 18 (vesicular monoamine), member 2 (Slc18a2, also known as vesicular monoamine transporter 2, or VMAT2), receptors (3/90, 3.3%) such as the alpha-5 nicotinic cholinergic receptor and dopamine receptor 2 (Drd2), or dopamine synthesis enzymes (2/90, 2.2%) such as TH and Ddc. These changes are likely due to loss of neurons in the SN due to tau, and validate the ability of AAV9 tau to produce a robust neuronal lesion. The overlap of tau's patterns relative to either GFP or empty vector support the argument that these are tau-specific changes. The significant changes in mRNAs for currently unnamed gene products are listed in Supplemental Table 3 for comparisons of the middle dose of AAV9 tau to either the middle dose AAV9 GFP or the AAV9 empty.

Dose-effects of AAV9 tau were examined across three doses spanning a 15-fold range and compared to vehicle injections. The lowest dose of AAV9 tau (2.4×10^9 vector genomes) had a modest effect, producing changes in 48 messages (22 mapped to identified genes), with the largest change a 4.14 fold decrease. On the other end, the highest dose (3.6×10^{10} vector genomes) had large effects, producing changes in 1679 messages, with the largest being a 131.84-fold increase. The messages that were affected by both the mid dose and high dose of AAV9 tau are listed in Table 3. There was no overlap in messages affected by the low dose and either the middle or high dose, with 45 specific messages affected by both the middle and high doses of tau (Table 3). Of those affected at both doses, 27 (60%) were involved in an immune response, and all were increased by tau. Other messages dose-dependently increased by tau include the microtubule components Tubb6, kinesin family member 20B (Kif20b), and kinesin family member 22 (Kif22; Mandelkow et al., 1995 for review), and the ubiquitin system enzymes Ube2l6 and a potential ubiquitin ligase (Herc6; Hochrainer et al., 2005). Messages decreased by both tau vector doses compared to vehicle include dopamine synthesis enzymes TH and Ddc, transporters DAT and VMAT2, and the alpha-6 nicotinic cholinergic receptor.

RT-PCR validated selected mRNAs from the microarray results. Primer/probe pairs were purchased for TH, DAT, and RT1-Db (antigen presentation molecule; Ettinger et al., 2004), as well as for pro-inflammatory cytokines interleukin 1 beta (IL-1β) and tumor necrosis factor-alpha (TNF), with glyceraldehyde 3-phosphate dehydrogenase (GAPDH) as the housekeeping gene. The groups examined were the vehicle control, the middle and high dose of AAV9 tau, and empty vector. There were no changes seen between the vehicle and the empty vector for any of the genes tested (data not shown). Fig. 2 shows mRNA levels normalized to GAPDH for the empty vector and two doses of tau vector. The data were analyzed by ANOVA/Bonferroni multiple comparisons (empty vector versus dose matched tau or mid versus high dose tau). For each target mRNA analyzed by RT-PCR, there were tau vector dose-dependent changes ($P < 0.05$-0.001), similar to the microarray results, with the high dose tau vector decreasing levels of TH and DAT and increasing levels of RT1-Db, IL-1B, and TNF.

Compared to mRNA changes reported to be caused by tau overexpression in tau transgenic mice (Chen et al., 2004; Ho et al., 2001), we found more changes, and of greater amplitude, in the course of two weeks of tau expression in rats. The genes reported from the tau transgenic mice did not appear on our lists, although differences in a number of factors,

including the time-course, the host species, the genotype of tau, and the brain region collected could have contributed.

Concomitant dopaminergic neuronal loss and microgliosis

Histological analysis of transgene expression, and effects on dopamine neurons and glia were performed with two subjects per group to mirror the microarray results at 2 weeks. There was visible GFP expression from the lowest dose (2.4×10^9 vg) in the SN pars compacta (Fig. 3A). Staining for the dopamine neuron marker TH in the substania nigra (Fig. 3B) appeared normal relative to uninjected controls (not shown). Staining for the microglial marker CD11b was limited to the needle track (Fig. 3C). With the middle dose (1.2×10^{10} vg), there was more robust GFP expression in neurons and their processes (Fig. 3D) compared to the low dose (Fig. 3A). Similar to the low dose GFP, the middle dose did not appear to alter TH staining in the SN (Fig. 3E) and microglial staining was limited to the needle track (Fig. 3F).

To monitor tau expression, we used the CP13 antibody specific for hyperphosphorylated tau, which provided a consistent subset of the staining for total human tau in this study and previously (Klein et al., 2009). At the lowest dose, hyperphosphorylated tau expression was detected in the SN (Fig. 3G), although TH immunoreactivity appeared to be unaffected (Fig. 3H) and microglial staining was limited to the needle track (Fig. 3I), as with the GFP vector injections. With the middle dose of tau vector, there was robust expression of hyperphosphorylated tau (Fig. 3J), with a blank area in the SN pars compacta, likely due to neuronal loss in that area, consistent with earlier findings (Klein et al., 2005; Klein et al., 2008; Klein et al., 2009). In terms of the transduction pattern, both the AAV9 GFP and AAV9 tau vectors produced transgene expression that was more limited to the pars compacta at the low dose and more widespread to the pars reticulata at the middle dose (pars reticulata GFP expression is not evident in Fig. 3D due to the camera exposure time), with no evidence of glial transduction, as found previously (Klein et al., 2008). The transduction pattern was therefore similar for either vector. The middle dose of tau vector resulted in loss of TH immunoreactivity in the SN (Fig 3K). The middle dose of tau vector induced microgliosis, with elevated CD11b immunoreactivity away from the needle track in the SN (Fig. 3L), in contrast to either dose of the GFP vector or the lower dose of tau vector. With the highest dose of tau vector (3.6×10^{10} vg), the loss of TH staining was more complete and the microgliosis even more pronounced (not shown). The dopaminergic cell loss and microgliosis mirrored each other, as only the middle dose of tau vector resulted in loss of TH immunoreactivity loss and increased microgliosis. Similar to the results with microglial staining, the middle dose of tau also led to an increase in staining for astroglia in the SN at 2 weeks (not shown). We performed time-course studies for the microgliosis comparing the middle dose of tau or GFP vectors with lactated ringer's vehicle injections at 1, 3, 7, and 14 days, and found pronounced microgliosis only at 14 days for the tau vector, with no signs of microgliosis away from the needle track with the controls at any of the intervals tested (Fig. S1). The microglial marker that we used, CD11b, is known as ITGAM (integrin alpha M) in the rat, but curiously, changes in ITGAM mRNA were not as consistently robust as observed with antibody detection of the protein. There was a greater level of ITGAM message with highest dose of tau vector relative to the mid dose (2.92 fold, $P = 0.003$), although when comparing the mid dose of tau to empty vector, there was only 1.60 fold more with the tau vector (not significant). The fact that the CD11b immunohistochemistry was noticeably elevated by the mid dose of tau vector at two weeks suggests either a greater sensitivity of the antibody technique or the possibility of post-transcriptional regulation.

Discussion

We studied gene transcript levels changed by human tau overexpression targeted to the rat SN to address processes by which the microtubule-associated protein tau can be toxic to neurons. Multiple groups, doses, and controls were studied. It was clear that the levels of transcripts for a number of pro-inflammatory markers were elevated specifically in response to tau, complementing the existing literature (Ishizawa et al., 2000; Yoshiyama et al., 2007; Klein et al., 2009) implicating inflammation as an important component of tau induced neurodegeneration. There were trends for tau vector dose-response in terms of tau expression, microgliosis, and dopaminergic cell loss, as well as for specific pro-inflammatory marker mRNAs in the microarray and RT-PCR (e.g., IL-1B and TNF). We hypothesize that the transcript profile largely reflects the gliosis induced by tau which peaked at two weeks when the RNA samples were collected, although both the tau expression and the neuronal loss also increase over this period. We correctly predicted specific message changes in dopaminergic neurons based on loss of neurons stained for TH after tau gene transfer (Klein et al., 2009). The lowest dose of AAV9 tau did not cause neuron loss or glial infiltration and served as a baseline, despite unequivocal tau expression. The highest dose of tau created a more complete lesion of the SN and the greatest reductions of dopaminergic mRNAs in the microarray. The tau vector dosing achieved baseline, partial, and nearly complete lesioning based on TH immunoreactivity. The middle tau vector dose decreased dopaminergic mRNAs, TH, Ddc, dopamine transporter (DAT), and the dopamine 2 receptor, and axon terminal loss was indicated by decreases for synaptic protein mRNAs such as synaptotagmin and alpha-synuclein. However, the study could neither determine changes that took place definitively in neurons versus glia, nor to directly attribute the inflammatory markers to the tau expression, or the gliosis or the neuronal loss, that was concomitantly caused by tau. More work would be needed to distinguish changes in neurons versus glia (i.e., laser capture microdissection) and to discern the sequence relative to injection, induction of expression, gliosis, and neuron loss.

With respect to the control vectors, the empty vector produced few changes compared to vehicle controls, affecting only 10 messages mildly, and did not increase any inflammatory markers. The AAV9 GFP produced more changes and of greater amplitude than the empty vector, and changes occurred in a variety of pathway categories. The trend of lowered endogenous rat tau mRNA could reflect neurotoxicity of the GFP, although TH immunohistochemistry appeared to be unaffected in the GFP group.

For the middle dose of tau vector, there was upregulation in many mRNAs involved in inflammation response relative to controls, including transcripts for leukocyte markers, chemokines, cytokine receptors, complement components, and interferon-inducible proteins. The control AAV9 injections of either the empty vector or the GFP vector to the SN of rats did not produce gliosis; there were a total of two immune related mRNA changes in the GFP group, and none in the empty vector group. We therefore believe that the changes in the middle and high dose tau vector groups are tau-specific, and not due to the AAV or the GFP. In terms of the potential relevance, gliosis and inflammation may occur at an early stage in the pathogenesis of PSP (Ishizawa et al., 2000). In tau transgenic mice, microgliosis precedes tangles and neuron loss (Yoshiyama et al., 2007), and in a tau transgenic rat model, inflammatory markers co-localize with degenerating axons (Zilka et al., 2009), suggesting that gliosis and inflammation may be underlying processes in tau neurofibrillary degeneration. Our previous study suggested that microgliosis was an early event in the progressing dopaminergic cell loss and motoric deficit, and was related to an augmented disease state in aged rats relative to young (Klein et al., 2009). The previous results along with the gliosis and upregulation of pro-inflammatory mRNAs in this study further implicate gliosis to be a key part of tau's neurotoxic mechanism. Our data are consistent with several

models studying the relationship of pro-inflammatory cytokines and tau pathology. Treatment of cultured neurons with TNF, or co-culturing activated microglia, induced tau aggregation in neurites (Gorlovoy et al., 2009). AAV-mediated overexpression of TNF in transgenic AD mice resulted in greater neuronal loss relative to controls (Janelsins et al., 2008). The anti-inflammatory drug minocycline reduced tau phosphorylation and insoluble aggregates in tau transgenic mice (Noble et al., 2009).

Upregulation of several components of the ubiquitin-proteasome pathway (see Oddo, 2008 for review) occurred, possibly connected to a compensatory mechanism to clear excess tau. These included the E2 conjugating enzymes Ube2n and Ube2l6, a potential E3 ligase Herc6, and proteasome subunits Psmb8 and Psmb9 (Lmp2) in various comparisons of tau versus controls. The proteasomal subunits Psmb8 and Psmb9 belong to the immunoproteasome which replace catalytic subunits of the proteasome when cells are exposed to pro-inflammatory cytokines IFN-gamma or TNF, and can accelerate the degradation of tau (Cardozo and Michaud, 2002). The immunoproteasome (for which Lmp2 is a marker) was reported to be upregulated in Alzheimer's and aged brains (Mishto et al., 2006). Another change that could be related to clearing excess tau was increased heat shock protein 1 (Hsp27), which has potential relevance to tau function (Shimura et al., 2004) and pathology (Sahara et al., 2007).

Aberrant cell-cycle re-entry has been hypothesized to contribute to tau neurodegeneration (see Lee et al., 2009 for review). We observed upregulation of mRNA for p21, a cell cycle inhibitor. In tau transgenic mice, p21 was found in the cytoplasm of neurons containing inclusions made of hyperphosphorylated tau (Delobel et al., 2006). However, our study could not distinguish whether the cell cycle mRNA changes occurred in tau transduced neurons, or the glia.

The tau gene transfer lowered mRNAs for dopaminergic markers and increased mRNAs for pro-inflammatory markers, which were validated by immunohistochemistry for TH or microglia, respectively. We titrated expression levels and tau-induced lesioning of dopaminergic neurons at an early time point of two weeks, which was concomitant with specific dose-dependent message changes. The profiling efforts after tau gene transfer in rats found gene expression changes that could be relevant to tau neurodegenerative diseases (Wakabayashi et al., 1994; Mirra et al., 1999; Di Maria et al., 2000; Poorkaj et al., 2002; Schneider et al., 2002), and one day lead to a specific gene product that could be rationally targeted.

Supplementary Material

Refer to Web version on PubMed Central for supplementary material.

Acknowledgments

Paula Polk performed the microarray procedures. NIH Grant NS048450 and Society for Progressive Supranuclear Palsy supported the research.

References

Buée L, Bussière T, Buée-Scherrer V, Delacourte A, Hof PR. Tau protein isoforms, phosphorylation and role in neurodegenerative disorders. Brain Res Brain Res Rev 2000;33:95–130. [PubMed: 10967355]

Cardozo C, Michaud C. Proteasome-mediated degradation of tau proteins occurs independently of the chemotrypsin-like activity by a nonprocessive pathway. Arch Biochem Biophys 2002;408:103–110. [PubMed: 12485608]

Chen F, Wollmer MA, Hoerndli F, Münch G, Kuhla B, Rogaev EI, Tsolaki M, Papassotiropoulos A, Götz J. Role of glyoxalase I in Alzheimer's disease. Proc Natl Acad Sci USA 2004;101:7687–7692. [PubMed: 15128939]

Delobel P, Lavenir I, Ghetti B, Holzer M, Goedert M. Cell cycle markers in a transgenic mouse model of human tauopathy: increased levels of cyclin-dependent kinase inhibitors p21Cip1 and p27Kip1. Am J Pathol 2006;168:878–887. [PubMed: 16507903]

Di Maria E, Tabaton M, Vigo T, Abbruzzese G, Bellone E, Donati C, Frasson E, Marchese R, Montagna P, Munoz DG, Pramstaller PP, Zanusso G, Ajmar F, Mandich P. Corticobasal degeneration shares a common genetic background with progressive supranuclear palsy. Ann Neurol 2000;47:374–377. [PubMed: 10716259]

Dufour JH, Dziejman M, Liu MT, Leung JH, Lane TE, Luster AD. IFN-gamma-inducible protein 10 (IP-10; CXCL10)-deficient mice reveal a role for IP-10 in effector T cell generation and trafficking. J Immunol 2002;168:3195–3204. [PubMed: 11907072]

Ettinger RA, Moustakas AK, Lobaton SD. Open reading frame sequencing and structure-based alignment of polypeptides encoded by RT1-Bb, RT1-Ba, RT1-Db, and RT1-Da alleles. Immunogenetics 2004;56:585–596. [PubMed: 15517241]

Gendron TF, Petrucelli L. The role of tau in neurodegeneration. Mol Neurodegener 2009;4:13. [PubMed: 19284597]

Golde TE. Disease modifying therapy for AD? J Neurochem 2006;99:689–707. [PubMed: 17076654]

Gorlovoy P, Larionov S, Pham TT, Neumann H. Accumulation of tau induced in neurites by microglial proinflammatory mediators. FASEB J 2009;23:2502–2513. [PubMed: 19289607]

Ho L, Xiang Z, Mukherjee P, Zhang W, De Jesus N, Mirjany M, Yemul S, Pasinetti GM. Gene expression profiling of the tau mutant (P301L) transgenic mouse brain. Neurosci Lett 2001;310:1–4. [PubMed: 11524143]

Hochrainer K, Mayer H, Baranyi U, Binder B, Lipp J, Kroismayr R. The human HERC family of ubiquitin ligases: novel members, genomic organization, expression profiling, and evolutionary aspects. Genomics 2005;85:153–164. [PubMed: 15676274]

Ishizawa K, Lin WL, Tiseo P, Honer WG, Davies P, Dickson DW. A qualitative and quantitative study of grumose degeneration in progressive supranuclear palsy. J Neuropathol Exp Neurol 2000;59:513–524. [PubMed: 10850864]

Janelsins MC, Mastrangelo MA, Park KM, Sudol KL, Narrow WC, Oddo S, LaFerla FM, Callahan LM, Federoff HJ, Bowers WJ. Chronic neuron-specific tumor necrosis factor-alpha expression enhances the local inflammatory environment ultimately leading to neuronal death in 3xTg-AD mice. Am J Pathol 2008;173:1768–1782. [PubMed: 18974297]

Klein RL, Dayton RD, Lin WL, Dickson DW. Tau gene transfer, but not alpha-synuclein, induces both progressive dopamine neuron degeneration and rotational behavior in the rat. Neurobiol Dis 2005;20:64–73. [PubMed: 16137567]

Klein RL, Dayton RD, Tatom JB, Diaczynsky CG, Salvatore MF. Tau expression levels from various adeno-associated virus serotypes produce graded neurodegenerative disease states. Eur J Neurosci 2008;27:1615–1625. [PubMed: 18380664]

Klein RL, Dayton RD, Diaczynsky CG, Wang DB. Pronounced microgliosis and neurodegeneration in aged rats after tau gene transfer. Neurobiol Aging. 2009 Epub ahead of print.

Kumar-Singh S, Van Broeckhoven C. Frontotemporal lobar degeneration: current concepts in the light of recent advances. Brain Pathol 2007;17:104–114. [PubMed: 17493044]

Lee HG, Casadesus G, Zhu X, Castellani RJ, McShea A, Perry G, Peterson RB, Bajic V, Smith MA. Cell cycle re-entry mediated neurodegeneration and its treatment role in the pathogenesis of Alzheimer's disease. Neurochem Int 2009;54:84–88. [PubMed: 19114068]

Ludolph AC, Kassubek J, Landwehrmeyer BG, Mandelkow E, Mandelkow EM, Burn DJ, Caparros-Lefebvre D, Frey KA, de Yebenes JG, Gasser T, Heutink P, Höglinger G, Jamrozik Z, Jellinger KA, Kazantsev A, Kretzschmar H, Lang AE, Litvan I, Lucas JJ, McGeer PL, Melquist S, Oertel W, Otto M, Paviour D, Reum T, Saint-Raymond A, Steele JC, Tolnay M, Tumani H, van Swieten JC, Vanier MT, Vonsattel JP, Wagner S, Wszolek ZK, Reisensburg Working Group for Tauopathies With Parkinsonism. Tauopathies with parkinsonism: clinical spectrum,

neuropathologic basis, biological markers, and treatment options. Eur J Neurol 2009;16:297–309. [PubMed: 19364361]

Martynoga B, Morrison H, Price DJ, Mason JO. Foxg1 is required for specification of ventral telencephalon and region-specific regulation of dorsal telencephalic precursor proliferation and apoptosis. Dev Biol 2005;283:113–127. [PubMed: 15893304]

Mandelkow E, Song YH, Schweers O, Marx A, Mandelkow EM. On the structure of microtubules, tau, and paired helical filaments. Neurobiol Aging 1995;16:347–354. [PubMed: 7566344]

Mirra SS, Murrell JR, Gearing M, Spillantini MG, Goedert M, Crowther RA, Levey AI, Jones R, Green J, Shoffner JM, Wainer BH, Schmidt ML, Trojanowski JQ, Ghetti B. Tau pathology in a family with dementia and a P301L mutation in tau. J Neuropathol Exp Neurol 1999;58:335–345. [PubMed: 10218629]

Mishto M, Bellavista E, Santoro A, Stolzing A, Ligorio C, Nacmias B, Spazzafumo L, Chiappelli M, Licastro F, Sorbi S, Pession A, Ohm T, Grune T, Franceschi C. Immunoproteasome and LMP2 polymorphism in aged and Alzheimer's disease brains. Neurobiol Aging 2006;27:54–66. [PubMed: 16298241]

Noble W, Garwood C, Stephenson J, Kinsey AM, Hanger DP, Anderton BH. Minocycline reduces the development of abnormal tau species in models of Alzheimer's disease. FASEB J 2009;23:739–750. [PubMed: 19001528]

Oddo S. The ubiquitin-proteasome system in Alzheimer's disease. J Cell Mol Med 2008;12:363–373. [PubMed: 18266959]

Paxinos, G.; Watson, C. The Rat Brain in Stereotaxic Coordinates. Academic Press; San Diego: 1998.

Poorkaj P, Muma NA, Zhukareva V, Cochran EJ, Shannon KM, Hurtig H, Koller WC, Bird TD, Trojanowski JQ, Lee VM, Schellenberg GD. An R5L tau mutation in a subject with a progressive supranuclear palsy phenotype. Ann Neurol 2002;52:511–516. [PubMed: 12325083]

Rolstad B, Vaage JT, Naper C, Lambracht D, Wonigeit K, Joly E, Butcher GW. Positive and negative MHC class I recognition by rat NK cells. Immunol Rev 1997;155:91–104. [PubMed: 9059885]

Sahara N, Maeda S, Yoshiike Y, Mizoroki T, Yamashita S, Murayama M, Park JM, Saito Y, Murayama S, Takashima A. Molecular chaperone-mediated tau protein metabolism counteracts the formation of granular tau oligomers in human brain. J Neurosci Res 2007;85:3098–3108. [PubMed: 17628496]

Schneider JA, Bienias JL, Gilley DW, Kvarnberg DE, Mufson EJ, Bennett DA. Improved detection of substantia nigra pathology in Alzheimer's disease. J Histochem Cytochem 2002;50:99–106. [PubMed: 11748299]

Shimura H, Miura-Shimura Y, Kosik KS. Binding of tau to heat shock protein 27 leads to decreased concentration of hyperphosphorylated tau and enhanced cell survival. J Biol Chem 2004;279:17957–17962. [PubMed: 14963027]

Song DY, Yang YC, Shin DH, Sugama S, Kim YS, Lee BH, Joh TH, Cho BP. Axotomy-induced dopaminergic neurodegeneration is accompanied with c-Jun phosphorylation and activation transcription factor 3 expression. Exp Neurol 2008;209:268–278. [PubMed: 18036593]

Wakabayashi K, Oyanagi K, Makifuchi T, Ikuta F, Homma A, Homma Y, Horikawa Y, Tokiguchi S. Corticobasal degeneration: etiopathological significance of the cytoskeletal alterations. Acta Neuropathol 1994;87:545–553. [PubMed: 8091948]

Yoshiyama Y, Higuchi M, Zhang B, Huang SM, Iwata N, Saido TC, Maeda J, Suhara T, Trojanowski TQ, Lee VM. Synapse loss and microglial activation precede tangles in a P301S tauopathy mouse model. Neuron 2007;53:337–351. [PubMed: 17270732]

Zilka N, Stozicka Z, Kovac A, Pilipcinec E, Bugos O, Novak M. Human misfolded truncated tau protein promotes activation of microglia and leukocyte infiltration in the transgenic rat model of tauopathy. J Neuroimmunol 2009;209:16–25. [PubMed: 19232747]

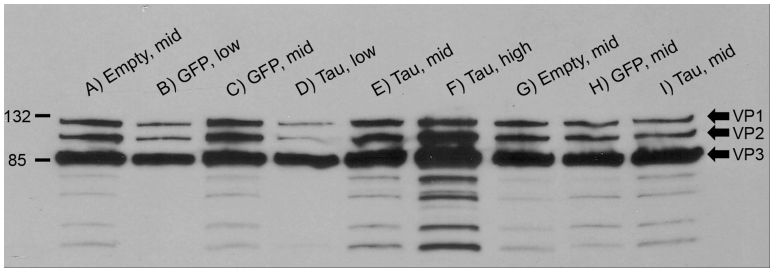

Fig 1.

AAV capsid protein western blot. Each viral dose used in the study was loaded and probed with an antibody against the AAV viral proteins VP1, VP2, and VP3 (indicated on right side of panel; size markers in kDa on left side), to ensure equal viral particles for the microarray study. Each matching dose of specific vectors had similar bands, and the intensity of the bands matched with the vector genome amounts loaded.

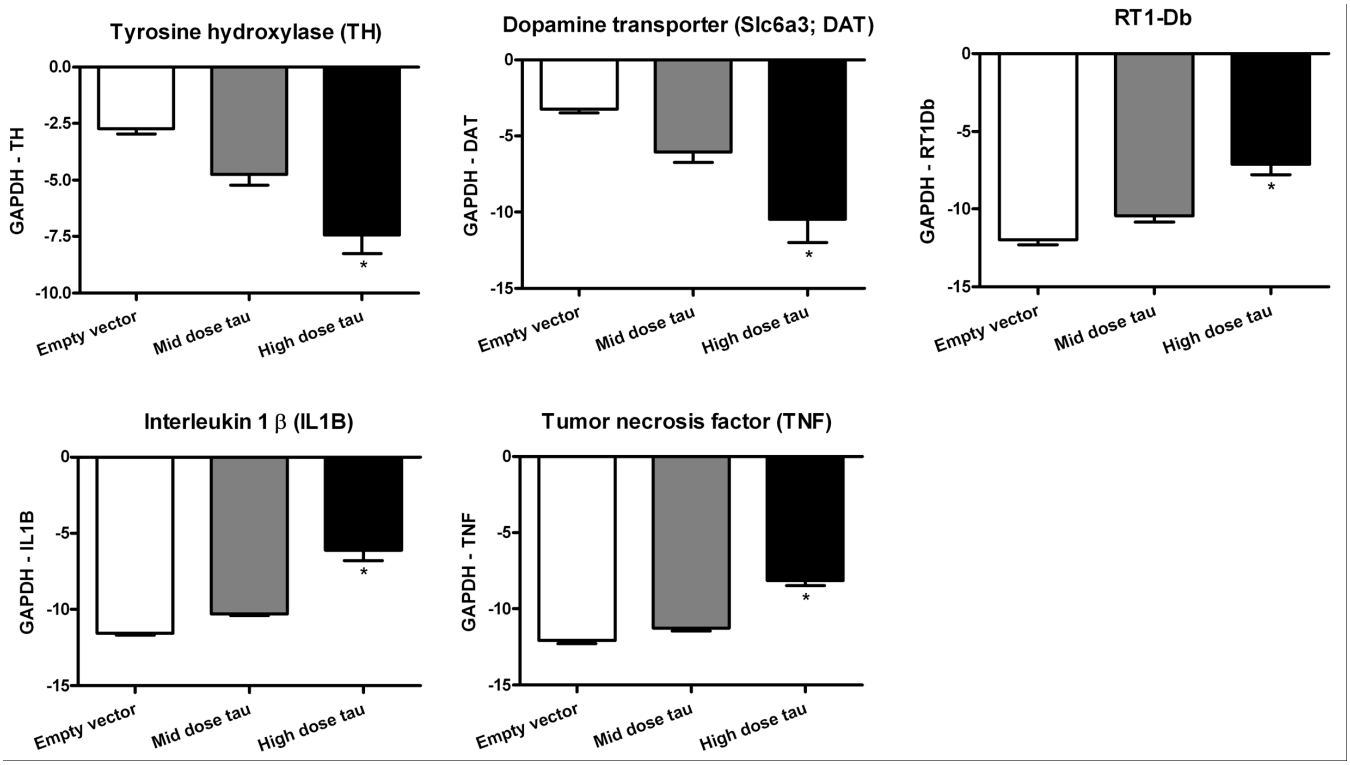

Fig 2.

RT-PCR validation of selected mRNAs from the microarray study: tyrosine hydroxylase (TH), dopamine transporter (DAT), RT1-Db (involved in antigen presentation), interleukin 1β (IL 1B), tumor necrosis factor (TNF). The amount of each target mRNA was normalized by subtracting the signal for a housekeeping mRNA (glyceraldehyde 3-phosphate dehydrogenase, GAPDH) from an aliquot of the same sample. Data are shown for the dose matching empty vector and tau groups (1.2×10^{10} vector genomes) and a higher dose of tau vector (3.6×10^{10} vector genomes) with 3-4 animals per group. In all cases, there were group differences by ANOVA with dose-dependent differences between the tau groups in Bonferroni post-tests (TH, DAT, $P < 0.05$; RT1-Db, $P < 0.01$; IL-1β, TNF, $P < 0.001$). High dose tau vector caused decreases in TH and DAT and increases in RT1-Db, IL-1B, and TNF, although all of the data are expressed as negative values as a result of the high levels of GAPDH.

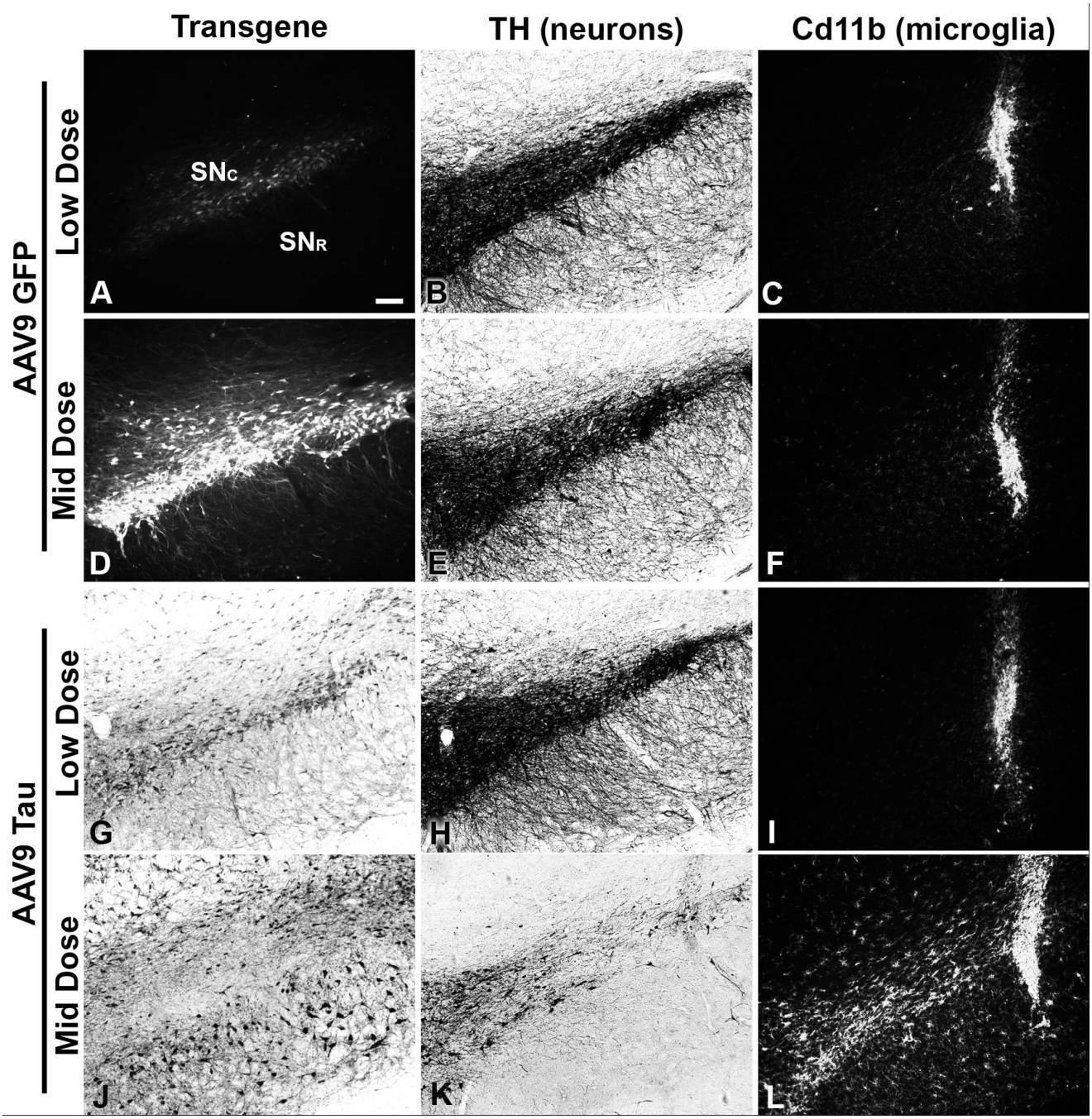

Fig 3.

Histological analyses two weeks after injections of AAV9 GFP or AAV9 tau to the substantia nigra (SN). Results from the low and mid doses of the microarray study (2.4×10^9 or 1.2×10^{10} vector genomes) are shown for each vector. (A-C) GFP epifluorescence, TH immunoreactivity, and staining for the microglial marker Cd11b on adjacent sections after low dose AAV9 GFP injection. TH staining was similar to the uninjected contralateral side (not shown), and pronounced microglial staining was restricted to the needle track. Labels for the SN pars compacta and pars reticulata are provided in A. (D-F) There was an apparent dose-dependent increase in both the spread and intensity of GFP expression with the higher dose, although both TH and Cd11b staining were similar at both doses of AAV9

GFP. (G-I) Hyperphosphorylated tau immunoreactivity (CP13 antibody) after AAV9 tau injection was found mainly in the SN pars compacta, and both TH and Cd11b staining appeared similar to results with both doses of the GFP vector. (J-L) In contrast, the higher dose of tau resulted in spread of hyperphosphorylated tau into the pars reticulata, but the pars compacta was partially blank for tau staining, likely due to dopaminergic cell loss in that area, consistent with reduced TH immunoreactivity in the SN. The microglial staining pattern was distinct with the higher dose of tau, with clear microgliosis away from the needle track in the SN. A higher dose of AAV9 tau (3.6×10^{10} vector genomes) resulted in even more pronounced effects on TH and Cd11b (not shown). Camera settings for the fluorescent images in A, D or C, F, I, L were kept equal. Bar in A = 134 μm.

Table 1

Messages changed by AAV9 tau relative to AAV9 GFP at the middle dose of 1.2×10^{10} vector genomes at two weeks.

Function	Gene Identifier	Gene Name	Gene ID	Fold change	Direction
Immune Response	U22520	Chemokine (C-X-C motif) ligand 10	Cxcl10	16.05	Up
	NM_017143	Coagulation factor X	F10	10.29	Up
	AA819034	Putative ISG12(b) protein	isg12(b)	8.83	Up
	AF068268	2-5 oligoadenylate synthetase 1B	Oas1b	7.19	Up
	AI409634	Radical S-adenosyl methionine domain containing 2	Rsad2	6.49	Up
	AW531805	Interferon-induced protein with tetratricopeptide repeats 3	Ifit3	5.1	Up
	BE096523	Interferon, alpha-inducible protein (clone IFI-15K)	G1p2	5.04	Up
	Z18877	2-5 oligoadenylate synthetase 1A	Oas1a	4.52	Up
	BI303379	Tumor necrosis factor receptor superfamily, member 12a	Tnfrsf12a	4.2	Up
	BI279526	RT1 class II, locus Db1	RT1-Db1	3.59	Up
	AA819629	Histocompatibility 28	H28	3.45	Up
	BF411036	Interferon regulatory factor 7	Irf7	3.39	Up
	NM_134350	Myxovirus (influenza virus) resistance 2	Mx2	3.38	Up
	BG378630	Placenta-specific 8	Plac8	3.34	Up
	AA892854	Chemokine (C-X-C motif) ligand 13	Cxcl13	3.27	Up
	Y00480	Histocompatibility 2, class II antigen E alpha	H2-Ea	3.22	Up
	NM_013069	Cd74 molecule, major histocompatibility complex, class II invariant chain	Cd74	3.04	Up
	BM390144	Arachidonate 12-lipoxygenase	Alox12	2.92	Up
	AI009765	Interferon-induced protein with tetratricopeptide repeats 2	Ifit2	2.86	Up
	NM_133624	Guanylate binding protein 2	Gbp2	2.73	Up
	BM382822	Intercellular adhesion molecule 5, telencephalin	Icam5	4.47	Down
Lipid Regulation	AI180413	Apolipoprotein H (beta-2-glycoprotein I)	Apoh	3.29	Up
	AW435376	Low density lipoprotein receptor-related protein 5	Lrp5	2.79	Up
	NM_012598	Lipoprotein lipase	Lpl	3.56	Down
	NM_013126	Diacylglycerol kinase, gamma	Dgkg	2.79	Down
	AI411493	Acyl-CoA thioesterase 4	Acot4	2.76	Down
Gene Regulation	NM_012912	Activating transcription factor 3	Atf3	5.21	Up
	NM_017103	Transcription elongation factor B (SIII), polypeptide 3	Tceb3	3.32	Up
	BM391471	Activating transcription factor 5	Atf5	2.83	Up

Function	Gene Identifier	Gene Name	Gene ID	Fold change	Direction
	BF402458	Zinc finger protein 667	Znf667	6.13	Down
Cell cycle/DNA repair	NM_024127	Growth arrest and DNA-damage-inducible, alpha	Gadd45a	3.06	Up
	U24174	Cyclin-dependent kinase inhibitor 1A (p21, Cip1)	Cdkn1a	2.87	Up
	AI010427	Cyclin-dependent kinase inhibitor 1A (p21, Cip1)	Cdkn1a	2.74	Up
	BF402732	Stromal antigen 2	Stag2	3	Down
Receptors	NM_024483	Adrenergic, alpha-1D-, receptor	Adra1d	5.4	Down
	NM_017078	Cholinergic receptor, nicotinic, alpha 5	Chrna5	3.36	Down
	NM_057184	Cholinergic receptor, nicotinic, alpha 6	Chrna6	2.92	Down
Transporter	NM_130748	Solute carrier family 38, member 4	Slc38a4	4.95	Down
	M80233	Solute carrier family 6 (neurotransmitter transporter, dopamine), member 3	Slc6a3	3.76	Down
	AF070475	Solute carrier family 4, sodium bicarbonate cotransporter, member 7	Slc4a7	3.34	Down
Other	BI286387	Small proline-rich protein 1A-like	Sprr1al	11.51	Up
	NM_133523	Matrix metallopeptidase 3	Mmp3	4.81	Up
	AB023896	Endothelin converting enzyme-like 1	Ecel1	3.78	Up
	AA892813	Muscleblind-like 2	Mbnl2	3.06	Up
	NM_017180	Pleckstrin homology-like domain, family A, member 1	Phlda1	2.8	Up
	AI317842	Kinesin family member 22	Kif22	2.76	Up
	NM_053955	Crystallin, mu	Crym	5.86	Down
	AF245172	Guanine deaminase	Gda	4.02	Down
	NM_031045	Inositol 1,4,5-trisphosphate 3-kinase A	Itpka	3.56	Down
	AW534032	Copine VII	Cpne7	3.4	Down

The top 50 greatest message changes (out of 166) associated with known proteins affected by AAV9 tau classified by function. N = 5/group.

Table 2

Messages changed by AAV9 tau relative to AAV9 empty at the middle dose of 1.2×10^{10} vector genomes at two weeks.

Function	Gene Identifier	Gene Name	Gene ID	Fold change	Direction
Immune response	AJ243338	RT1 class I, CE5	RT1-Aw2	16.3	Up
	U22520	Chemokine (C-X-C motif) ligand 10	Cxcl10	9.17	Up
	AA819034	Putative ISG12(b) protein	isg12(b)	8.86	Up
	X52711	Myxovirus (influenza virus) resistance 1	Mx1	7.79	Up
	AI409634	Radical S-adenosyl methionine domain containing 2	Rsad2	6.71	Up
	AW531805	Interferon-induced protein with tetratricopeptide repeats 3	Ifit3	5.71	Up
	BI303379	Tumor necrosis factor receptor superfamily, member 12a	Tnfrsf12a	5.5	Up
	BE096523	Interferon, alpha-inducible protein (clone IFI-15K)	G1p2	5.46	Up
	BF411036	Interferon regulatory factor 7	Irf7	5.16	Up
	NM_134350	Myxovirus (influenza virus) resistance 2	Mx2	4.88	Up
	AF068268	2-5 oligoadenylate synthetase 1B	Oas1b	4.75	Up
	BE118697	Interferon-induced protein with tetratricopeptide repeats 2	Ifit2	4.73	Up
	Z18877	2-5 oligoadenylate synthetase 1A	Oas1a	3.99	Up
	BG378630	Placenta-specific 8	Plac8	3.81	Up
	NM_017143	Coagulation factor X	F10	3.56	Up
	AI009765	Interferon-induced protein with tetratricopeptide repeats 2	Ifit2	3.48	Up
	NM_133624	Guanylate nucleotide binding protein 2	Gbp2	3.07	Up
	BI296385	Chemokine (C-X-C motif) ligand 16	Cxcl16	2.95	Up
	AF065438	Lectin, galactoside-binding, soluble, 3 binding protein	Lgals3bp	2.74	Up
	BM391818	2 -5 oligoadenylate synthetase 1I	Oas1i	2.73	Up
	Y00480	RT1 class II, locus Da	RT1-Da	2.71	Up
	AW915763	Serine (or cysteine) peptidase inhibitor, clade G, member 1	Serping1	2.62	Up
	BG378249	RT1 class II, locus Ba	RT1-Ba	2.61	Up
	BI292425	Complement component 1, r subcomponent	C1r	2.59	Up
	AI011757	Fc fragment of IgG, low affinity IIIa, receptor	Fcgr3a	2.56	Up
	AI011393	Fc receptor-like S, scavenger receptor	Fcrls	2.55	Up
Transporter	M80233	Solute carrier family 6 (neurotransmitter transporter, dopamine), member 3	Slc6a3	6.61	down
	NM_013031	Solute carrier family 18 (vesicular monoamine), member 2	Slc18a2	5.51	down
	NM_012694	Solute carrier family 6 (neurotransmitter transporter, dopamine), member 3	Slc6a3	5.47	down

Function	Gene Identifier	Gene Name	Gene ID	Fold change	Direction
	M97381	Solute carrier family 18 (vesicular monoamine), member 2	Slc18a2	3.93	down
	AF070475	Solute carrier family 4, sodium bicarbonate cotransporter, member 7	Slc4a7	3.5	down
Cell cycle/DNA repair	AI010427	Cyclin-dependent kinase inhibitor 1A	Cdkn1a	3.84	Up
	U24174	Cyclin-dependent kinase inhibitor 1A	Cdkn1a	3.32	Up
	NM_024127	Growth arrest and DNA-damage-inducible 45 alpha	Gadd45a	2.75	Up
	BI285978	Poly (ADP-ribose) polymerase family, member 12	Parp12	2.6	Up
Dopamine	NM_012740	Tyrosine hydroxylase	Th	3.26	down
	U31884	Dopa decarboxylase	Ddc	2.36	down
Other	NM_012912	Activating transcription factor 3	Atf3	7.24	up
	AA819788	Receptor transporter protein 4	Rtp4	4.35	Up
	AI502796	Coiled-coil domain containing 109B	Ccdc109b	3.57	up
	AA943147	Potential ubiquitin ligase	Herc6	3.3	Up
	AB023896	Endothelin converting enzyme-like 1	Ecel1	3.14	up
	AI180413	Apolipoprotein H	Apoh	2.67	up
	AA945955	Osteoglycin	Ogn	2.61	up
	NM_080767	Proteasome (prosome, macropain) subunit, beta type 8	Psmb8	2.55	Up
	NM_017078	Cholinergic receptor, nicotinic, alpha polypeptide 5	Chrna5	3.56	down
	AW434432	Opsin 4 (melanopsin)	Opn4	2.79	down
	BI286396	PERP, TP53 apoptosis effector	Perp	2.87	down
	NM_053744	Delta-like 1 homolog (Drosophila)	Dlk1	2.68	down
	AW534032	Copine VII	Cpne7	2.54	down

The top 50 greatest message changes (out of 90) associated with known proteins affected by AAV9 tau classified by function. N = 5/group.

Table 3

Messages dose-dependently changed by AAV9 tau.

				Fold change		
Function	**Gene Identifier**	**Gene Name**	**Gene ID**	**Mid dose**	**High dose**	**Direction**
Immune Response	AI409634	Radical S-adenosyl methionine domain containing 2	Rsad2	6.04	29.56	Up
	U22520	Chemokine (C-X-C motif) ligand 10	Cxcl10	5.98	78.36	Up
	AA819034	Putative ISG12(b) protein	isg12(b)	5.46	60.24	Up
	X52711	Myxovirus (influenza virus) resistance 1	Mx1	5.11	54.18	Up
	BE096523	Interferon, alpha-inducible protein (clone IFI-15K)	G1p2	5	38.42	Up
	AF068268	2-5 oligoadenylate synthetase 1B	Oas1b	4.83	14.01	Up
	AW531805	Interferon-induced protein with tetratricopeptide repeats 3	Ifit3	4.16	38.5	Up
	Z18877	2-5 oligoadenylate synthetase 1A	Oas1a	3.85	19.91	Up
	BF411036	Interferon regulatory factor 7	Irf7	3.37	34.23	Up
	BM391818	2 -5 oligoadenylate synthetase 1I	Oas1i	3.29	9.09	Up
	NM_017143	Coagulation factor X	F10	3.28	29.13	Up
	AI009765	Interferon-induced protein with tetratricopeptide repeats 2	Ifit2	3.27	14.48	Up
	NM_134350	Myxovirus (influenza virus) resistance 2	Mx2	3.18	23.12	Up
	AJ243338	RT1 class Ib, locus Aw2	RT1-Aw2	3.06	62.81	Up
	BI296097	Interferon stimulated exonuclease 20	Isg20	2.74	10.93	Up
	AA819629	Histocompatibility 28	H28	2.73	19.54	Up
	BF417541	DEXH (Asp-Glu-X-His) box polypeptide 58	Dhx58	2.65	21.19	Up
	NM_133298	Glycoprotein (transmembrane) nmb	Gpnmb	2.57	8.84	Up
	AI407339	Immunity-related GTPase family, M	Irgm	2.5	14.3	Up
	AF065438	Lectin, galactoside-binding, soluble, 3 binding protein	Lgals3bp	2.38	18.41	Up
	BG378630	Placenta-specific 8	Plac8	2.35	35.32	Up
	NM_053736	Caspase 4, apoptosis-related cysteine peptidase	Casp4	2.34	9.5	Up
	L40362	RT1 class Ib, locus Aw2	RT1-Aw2	2.27	25.21	Up
	M10072	Protein tyrosine phosphatase, receptor type, C	Ptprc	2.26	14	Up
	NM_031832	Lectin, galactoside-binding, soluble, 3	Lgals3	2.23	14.92	Up
	BI292425	Complement component 1, r subcomponent	C1r	2.09	9.55	Up
	NM_032612	Signal transducer and activator of transcription 1	Stat1	2.06	11.93	Up
Cytoskeleton	BI274903	Tubulin, beta 6	Tubb6	2.54	7.02	Up

Function	Gene Identifier	Gene Name	Gene ID	Fold change		Direction
				Mid dose	High dose	
	AI317842	Kinesin family member 22	Kif22	2.15	4.51	Up
	BE110723	Kinesin family member 20B	Kif20b	2.11	4.69	Up
Transporter	M80233	Solute carrier family 6 (neurotransmitter transporter, dopamine), member 3	Slc6a3	5.1	85.49	Down
	NM_012694	Solute carrier family 6 (neurotransmitter transporter, dopamine), member 3	Slc6a3	4.52	22.13	Down
	BF545691	Solute carrier family 18 (vesicular monoamine), member 2	Slc18a2	4.24	15.63	Down
Dopamine	NM_012740	Tyrosine hydroxylase	Th	2.81	10.91	Down
	U31884	Dopa decarboxylase (aromatic L-amino acid decarboxylase)	Ddc	2.36	5.95	Down
Ubiquitin	BI279216	Ubiquitin-conjugating enzyme E2L 6	Ube2l6	2.63	8.78	Up
	AA943147	Potential ubiquitin ligase	Herc6	2.49	5.82	Up
Other	NM_012912	Activating transcription factor 3	Atf3	8.04	17.47	Up
	AA819788	Receptor (chemosensory) transporter protein 4	Rtp4	2.87	16.67	Up
	NM_053819	TIMP metallopeptidase inhibitor 1	Timp1	2.68	13.27	Up
	BM389006	Thymidine kinase 1, soluble	Tk1	2.18	4.8	Up
	AA859235	Cell division cycle associated 7	Cdca7	2.01	4.39	Up
	NM_030847	Epithelial membrane protein 3	Emp3	2.03	5.5	Up
	AA819679	Poly (ADP-ribose) polymerase family, member 9	Parp9	2	10.24	Up
	NM_057184	Cholinergic receptor, nicotinic, alpha 6	Chrna6	2.62	6.95	Down

Messages associated with known proteins changed by both the middle and high doses of AAV9 tau (1.2 or 3.6 × 10^{10} vector genomes) relative to vehicle injections, and classified by function. N = 4-5/group.